*Int. J. Heat Mass Transfer.* Vol. 35, No. 2, pp. 525–532, 1992
Printed in Great Britain

0017–9310/92 $5.00 + 0.00


# Bifurcation analysis of pressure-drop oscillations and the Ledinegg instability

M. M. PADKI,† K. PALMER,‡ S. KAKAÇ† and T. N. VEZIROĞLU†

† Clean Energy Research Institute, University of Miami, Coral Gables, FL 33124, U.S.A.
‡ Department of Mathematics and Computer Science, University of Miami, Coral Gables, FL 33124, U.S.A.

(*Received* 5 *March* 1990 *and in final form* 11 *February* 1991)

**Abstract**—Pressure-drop oscillations and the Ledinegg instability are analyzed from the perspective of dynamical systems theory. An integral formulation is developed to model the two-phase flow system. Instability criteria independent of the actual two-phase flow model are derived for the two phenomena. It is shown that the pressure-drop oscillation limit-cycles occur after a super-critical Hopf bifurcation. In an extension of the analysis, an effort is made to clarify the mechanisms of the pressure-drop type oscillations and Ledinegg instability. The two phenomena are classified from the angle of bifurcation theory, and the differences are outlined.

## 1. INTRODUCTION

TWO-PHASE flow systems are prone to dynamic and static instabilities of many kinds [1, 2]. In the last few decades a considerable amount of research work has been carried out in this field all over the world, and most instabilities are more-or-less completely understood. This paper focuses on the pressure-drop oscillations, and aims at proving some theoretical results for these.

This work has been motivated principally by two ideas. The first source of motivation was the lack of the proof of existence and uniqueness of pressure-drop oscillations. The existence and uniqueness was shown for the case of density-wave oscillations, with the help of the Hopf-bifurcation theorem [3]. However, in the case of pressure-drop oscillations, the analytical proofs have been limited to showing that operation on the negative-slope region of the pressure-drop vs mass flow rate characteristics is unstable in the presence of a compressible volume upstream or within the flow circuit [1, 2]. The nonlinear stability analysis is carried a step further in this paper with the help of a simple model.

The second source of motivation was to develop a unified framework for analyzing the pressure-drop oscillations and the Ledinegg (excursive) instability. Both are caused by attempts to operate on the negative-slope region of the pressure-drop vs mass flow rate characteristics. However, the mechanisms for both are completely different. Thus it was also sought to clarify the differences between the two phenomena mathematically.

## 2. FORMULATION OF THE MODEL

### 2.1. *Integral formulation*

The governing equations are transient equations in one spatial dimension, and they are coupled to each other. In order to simplify the problem, the help of the integral method is sought. The integral method is one of the most powerful tools used for the purpose of reducing the dimensionality of complex problems. In essence, the integral method consists of integrating the governing equations over the domain of interest along one of the independent variables, so as to substitute the continuous dependence of parameters on that variable by an average dependence.

Figure 1 is a schematic diagram of the experimental apparatus, indicating the main variables of the mathematical analysis. The governing equations are integrated over the flow lengths (between the main and surge tanks, as well as between the surge tank and the exit), to get three coupled time-dependent (first-order, nonlinear) equations. The following assumptions are made:

(1) At any instant, the mass velocity is uniform in the two flow circuits; i.e. $G_i$ characterizes the mass velocity between the main tank and the surge tank (the 'external' circuit), and $G_o$ characterizes the mass velocity between the surge tank and the exit (the 'internal' circuit).

(2) The frictional resistance can be represented in terms of a friction factor similar to the Blasius, which can be obtained as a suitable function of the thermodynamic and flow properties.

(3) The total pressure-drop between the main and surge tank is assumed to be concentrated at the inlet restriction.

(4) The main tank and the system exit are maintained at constant pressures, $P_i$ and $P_e$, respectively. This corresponds closely to the actual experimental system.

The three equations are obtained as follows:

## NOMENCLATURE

| | |
|---|---|
| $D$ | inner diameter of the heater tube [m] |
| $Eu$ | Euler number, $P_o/(G_{oo}^2/\rho_l)$ [dimensionless] |
| $f$ | friction factor [dimensionless] |
| $F_m$ | two-phase flow friction multiplier [dimensionless] |
| $Fr$ | Froude number, $(G_{oo}^2/\rho_l)/(gL_v)$ [dimensionless] |
| $g$ | gravitational acceleration, $9.806\,m^2\,s^{-1}$ |
| $G$ | fluid mass velocity, $\rho u$ [$kg\,m^{-2}\,s^{-1}$] |
| $G_i$ | inlet fluid mass velocity into surge tank [$kg\,m^{-2}\,s^{-1}$] |
| $G_o$ | outlet fluid mass velocity from surge tank [$kg\,m^{-2}\,s^{-1}$] |
| $K_i$ | resistance coefficient for inlet restriction [dimensionless] |
| $P$ | surge tank pressure [Pa] |
| $P_e$ | exit pressure [Pa] |
| $P_i$ | main tank pressure [Pa] |
| $P_o$ | steady-state surge tank pressure [Pa] |
| $Q$ | heat input into the fluid [W] |
| $t$ | time [s] |
| $V_o$ | steady-state volume of the gas in the surge tank [$m^3$] |
| $x$ | quality of the liquid–vapor mixture [dimensionless]. |

Greek symbols

| | |
|---|---|
| $\Lambda$ | friction number, $2fL_2/D$ [dimensionless] |
| $\lambda$ | eigenvalues |
| $\rho$ | density [$kg\,m^{-3}$] |
| $\tau_{l1}$ | outer loop time constant, $\rho_l \cdot L_1/G_{oo}$ [s] |
| $\tau_{l2}$ | inner loop time constant, $\rho_l \cdot L_2/G_{oo}$ [s] |
| $\psi$ | void fraction [dimensionless]. |

Subscripts

| | |
|---|---|
| e | exit condition |
| f | fluid parameter |
| i | inlet condition |
| l | liquid |
| o | steady-state or operating condition |
| v | vapor, vertical. |

Inlet mass velocity

$$L_1 \frac{dG_i}{dt} = (P_i - P) - K_i \frac{G_i^2}{\rho_l}. \quad (1)$$

Surge tank dynamics [4]

$$\frac{dP}{dt} = P^2 \frac{(G_i - G_o)A_p}{P_o V_o \rho_l}. \quad (2)$$

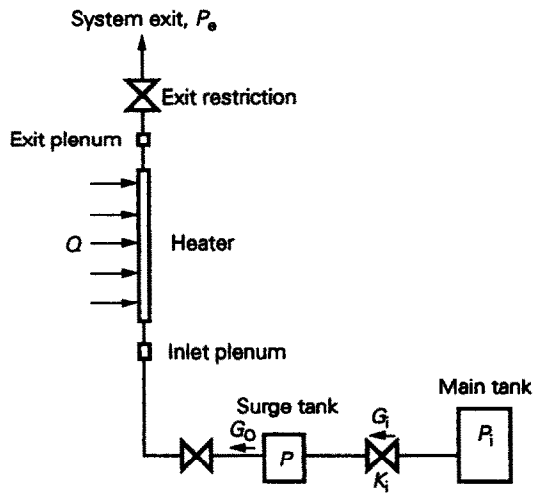


FIG. 1. Schematic diagram of the boiling flow system.

Outlet mass velocity

$$L_2 \frac{dG_o}{dt} = (P - P_e) - \rho_{av} g L_v - \frac{G_o^2}{\rho_l} \times \left\{ \frac{(1-x_e)^2}{(1-\psi_e)} + \frac{\rho_l x_e^2}{\rho_v \psi_e} - 1 + F_m + \frac{2fL_2}{D} \right\}. \quad (3)$$

The details of this derivation are presented in Appendix A.

In this equation, $F_m$ is the so-called two-phase flow multiplier, and takes care of the concentrated pressure-drop at the exit restriction. Typically, $F_m$ can be adequately represented as a quadratic or a cubic function of the exit quality [2]. For convenience, equation (3) is rewritten in the following compact notation:

$$L_2 \frac{dG_o}{dt} = (P - P_e) - f(G_o, Q) \frac{G_o^2}{\rho_l} \quad (4)$$

where

$$f(G_o, Q) \frac{G_o^2}{\rho_l} = \rho_{av} g L_v + \frac{G_o^2}{\rho_l} \times \left\{ \frac{(1-x_e)^2}{(1-\psi_e)} + \frac{\rho_l x_e^2}{\rho_v \psi_e} - 1 + F_m + \frac{2fL_2}{D} \right\}. \quad (5)$$

### 2.2. *Nonlinear simulation of pressure-drop oscillations*

The model presented by equations (1)–(3) is validated first with respect to experimental results. The solution at the operating point is computed by setting the time derivatives to zero. Then the inlet mass velocity is perturbed, and the equations are integrated simultaneously using the fourth-order Runge–Kutta

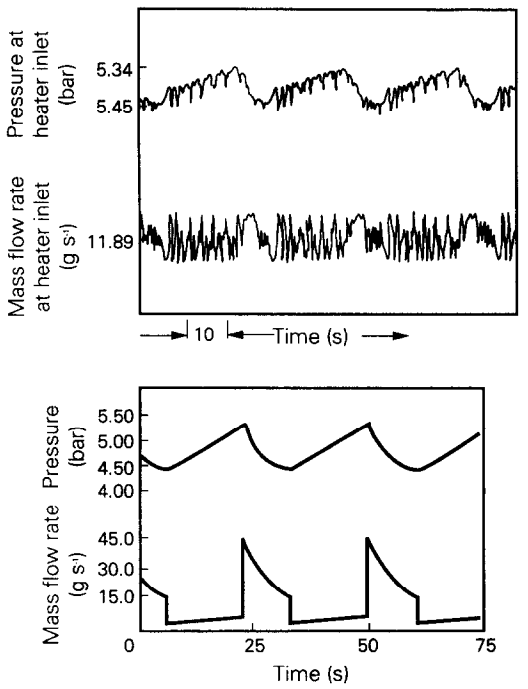


FIG. 2. Sample oscillation results: comparison with experimental results. Heat input $Q = 400$ W, inlet liquid (Freon-11) temperature = 23°C, operating mass flow rate = 11.89 g $s^{-1}$, heater: coated nichrome, i.d. = 7.5 mm, o.d. = 9.5 mm.

scheme, to give rise to the pressure-drop oscillations. Figure 2 shows a sample of the predicted wave-forms of the pressure-drop oscillations, along with experimentally obtained recordings. The experimental results are taken from ref. [5]. It can be seen that despite the simplicity of the model, the essence of the pressure-drop oscillations is captured. (The superimposed high-frequency oscillations seen in the experimental results are the so-called density-wave oscillations, which result from delays in kinematic wave propagation. The present model is not designed to handle these.)

### 2.3. *Nondimensionalization of governing equations*

It is convenient to nondimensionalize equations (1)–(3) of the model using the following scale parameters, namely, the surge tank pressure and the mass velocity at the operating point:

(i) pressure: $P_o$;
(ii) mass velocity: $G_{oo}$;

to get the following:

$$\frac{d\bar{G}_i}{d\tau} = A[Eu(\bar{P}_i - \bar{P}) - K_i\bar{G}_i^2] \tag{6}$$

$$\frac{d\bar{P}}{d\tau} = \bar{P}^2(\bar{G}_i - \bar{G}_o) \tag{7}$$

$$\frac{d\bar{G}_o}{d\tau} = B[Eu(\bar{P} - \bar{P}_e) - f(\bar{G}_o, Q)\bar{G}_o^2] \tag{8}$$

where $f(\bar{G}_o, Q)$ is the nondimensionalized total pressure-drop in the heated channel, expressed as

$$f(\bar{G}_o, Q) = \frac{\rho_{av}}{\rho_l}\frac{1}{Fr} - \left\{\frac{(1-x_e)^2}{(1-\psi_e)} + \frac{\rho_l x_e^2}{\rho_v \psi_e} - 1 + F_m + \Lambda\right\}. \tag{9}$$

The overbars indicate the nondimensional quantities, and $Eu(= P_o/(G_{oo}^2/\rho_l))$, $Fr(= (G_{oo}^2/\rho_l)/(gL_v))$ and $\Lambda(= 2fL_2/D)$ are the Euler number, Froude number and friction number, respectively.

The average density over the vertical segment of the loop is

$$\rho_{av} = \frac{1}{L_v}\int_0^{L_v} \rho\, dz.$$

Also, $\tau(= t/\tau_s)$ is the nondimensional time, and

$$A = \frac{\tau_s}{\tau_{l1}} \quad \text{and} \quad B = \frac{\tau_s}{\tau_{l2}}$$

where $\tau_s(= V_o\rho_l/A_pG_{oo})$ is the time constant of the surge tank, and $\tau_{l1}(= \rho_l \cdot L_1/G_{oo})$ and $\tau_{l2}(= \rho_l \cdot L_2/G_{oo})$ are the outer and inner loop time constants, respectively.

The time, $t$, in these equations is nondimensionalized with respect to $\tau_s$, since experimental evidence suggests that the time period of pressure-drop oscillations is a function of the time constant of the surge tank.

This scheme of nondimensionalization is similar to that used in ref. [3].

## 3. BIFURCATION ANALYSIS

### 3.1. *Linearized stability analysis*

To analyze the stability of the system of equations developed in the last section, we first form the Jacobian of the system, evaluate it at the operating point and find the eigenvalues of this Jacobian. The nature and signs of the eigenvalues allow us to draw important conclusions about the stability of the solution, as well as about the expected solution in the unstable region [6, 7]. At the operating point, $\bar{G}_i = \bar{G}_o = \bar{P} = 1$, and the characteristic equation is formulated as

$$\lambda^3 + e_1\lambda^2 + e_2\lambda + e_3 = 0 \tag{10}$$

where

$$e_1 = 2AK_i + B\left[\frac{df(1,Q)}{d\bar{G}_o} + 2f(1,Q)\right] \tag{11}$$

$$e_2 = (A+B)Eu + 2ABK_i\left[\frac{df(1,Q)}{d\bar{G}_o} + 2f(1,Q)\right] \tag{12}$$

$$e_3 = ABEu\left[2K_i + \frac{df(1,Q)}{d\bar{G}_o} + 2f(1,Q)\right]. \tag{13}$$

Stability of the system of equations is assured when real parts of all eigenvalues are negative. A possible bifurcation point—where the nature of the solution shows a qualitative change, e.g. from a stable point to a limit cycle—is located by identifying a root of the characteristic equation for which the real part is zero [7]. To locate the bifurcation points of the present system, we use the Hurwitz theorem, which states that the necessary and sufficient conditions for the real parts of all eigenvalues to be negative are [8]:

(a) $e_1 > 0$, which leads to

$$2AK_i + B\left[\frac{df(1,Q)}{d\bar{G}_o} + 2f(1,Q)\right] > 0;$$

(b) $(e_1e_2 - e_3) > 0$, to be taken up in the next subsection; and

(c) $e_3(e_1e_2 - e_3) > 0$, which results in

$$\left[2K_i + 2f(1,Q) + \frac{df(1,Q)}{d\bar{G}_o}\right] > 0.$$

When $A = B$ (a good approximation of our experimental set-up), criteria (a) and (c) become identical, and can be rewritten as

$$\text{(d)} \qquad \left[2f(1,Q) + \frac{df(1,Q)}{d\bar{G}_o}\right] > -2K_i \qquad (14)$$

and criterion (b) simplifies to

$$\text{(e)} \qquad \left[2f(1,Q) + \frac{df(1,Q)}{d\bar{G}_o}\right] > \frac{1}{2}\frac{-Eu}{K_iA}. \qquad (15)$$

In this way, we have obtained criteria for stable operation of the given system. The point to be emphasized here is that *these criteria are independent of the actual two-phase flow model used*; which means that they can be used for, say, graphical determination of instability thresholds, based on experimental data.

Towards this end, criteria (14) and (15) are reconverted to the dimensional form, and written in terms of the slopes of the steady-state pressure-drop vs mass flow rate characteristics. Figure 3 is plotted to check the theoretical predictions of the instability thresholds against experimental results. These thresholds are determined by actually measuring the slopes, and comparing the value with that obtained by the stability criterion (b). In the case of our experimental conditions—i.e. with main tank and exit pressures maintained at about 7 and 1.5 bar, respectively—the criteria for *instability* can be calculated to be of the following orders (in terms of the scales of Fig. 3):

$$\frac{dP}{d\dot{m}} < -0(10^{-5})\ \text{bar}\,(\text{g s}^{-1})^{-1} \text{ for criterion (15)}$$

(pressure-drop oscillations)

and

$$\frac{dP}{d\dot{m}} < -0(10^{-1})\ \text{bar}\,(\text{g s}^{-1})^{-1} \text{ for criterion (14)}$$

(Ledinegg instability).

The model predictions can be seen to be in good agreement with the experimental results.

It is to be noted at this point that $f(1, Q)$ is always a positive number; however, with the addition of more and more heat into the system, the slope, i.e. $df(1, Q)/d\bar{G}_o$, becomes more and more negative and leads to various bifurcations. When there is no heat input into the system, this slope is zero, and all stability conditions are identically satisfied—which confirms the common knowledge that single-phase systems are always stable. It is easy to see that, as $Q$ is increased from zero, the Hopf bifurcation occurs first. The saddle-node bifurcation occurs with further addition of heat, when the internal characteristics become steeper than the external. As shown in Appendix B, criterion (c) corresponds to a saddle-node bifurcation (analogous to a Ledinegg bifurcation). We now proceed to analyze criterion (b).

### 3.2. *Existence and uniqueness of pressure-drop oscillation limit cycles*

To prove the existence and uniqueness of these oscillations, we use the Hopf bifurcation theorem, proved by Hopf in 1942 [8]. An important question concerns the choice of the bifurcation parameter. It is well known that increasing the heat input, $Q$, into the system makes the slope of the pressure-drop characteristics more negative, and also that the pressure-drop oscillations are connected with this slope. Therefore, we choose $Q$ as the bifurcation parameter.

In the limiting case of stability, the inequality in (b) can be substituted by an equality. Using that relation, the main characteristic equation can be factorized to give

$$(\lambda + e_1)(\lambda^2 + e_2) = 0 \qquad (16)$$

leading to

$$\lambda_1 = -e_1 \qquad (17)$$

and

$$\lambda_{2,3} = \pm\sqrt{(-e_2)}. \qquad (18)$$

Since $e_2$ is positive, a pair of eigenvalues crosses the imaginary axis at the point of incipient loss of stability. Differentiating equation (10) with respect to the bifurcation parameter, we can evaluate $\partial\lambda_r/\partial Q$, which can be shown to be

$$\frac{\partial\lambda_r}{\partial Q} = \frac{-1}{2(e_1^2 + e_2)}\frac{\partial}{\partial Q}(e_1e_2 - e_3). \qquad (19)$$

The derivative of $(e_1e_2 - e_3)$ is negative, since initially this quantity is greater than zero (e.g. when there is no heat input into the system); at the bifurcation point it is zero; and later becomes negative. Thus the eigenvalues cross the imaginary axis with positive speed.

Finally, we show that this bifurcation is super-critical, i.e. the periodic solutions lie on the unstable side. This would imply that the limit cycles are stable, and

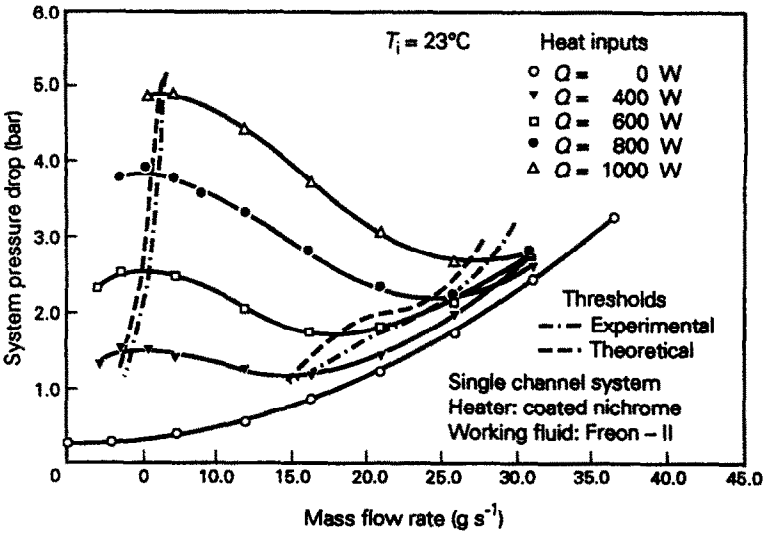


FIG. 3. Prediction of the thresholds of instability. Comparison with experimental results.

all solutions would tend toward it for given operating conditions [3]. In order to show this exactly, we would need to reduce the given system of equations using the center-manifold theory and then compute higher derivatives. However, since the derivative of the function, $f(\bar{G}_o, Q)$ (the nondimensionalized total pressure-drop in the heated channel), is not continuous at two points (namely, at exit quality 0 and 1), it is not possible to perform these calculations. Therefore, we rely on indirect methods to show the super-criticality of the bifurcation; specifically, we show that the amplitude of the oscillations grows as heat input is increased past the bifurcation point.

Figure 4 shows the experimental results for the variation of the amplitude of oscillations with heat input (taken from ref. [5]). It is evident that the amplitude increases roughly as the square root of the difference between the heat input and the heat input at the bifurcation point (as shown by the fitted curve in the figure). Figure 5 shows the results of the present integral model for the variation of the oscillation amplitudes very close to the bifurcation point. (This is shown because experimental data close to the bifurcation point are not available.) Again, it is evident that, very close to the bifurcation point, the amplitude grows as heat input is increased, and that it has a square-root relationship with the heat input. Based on these two pieces of data, we can conclude that it is indeed a super-critical Hopf bifurcation.

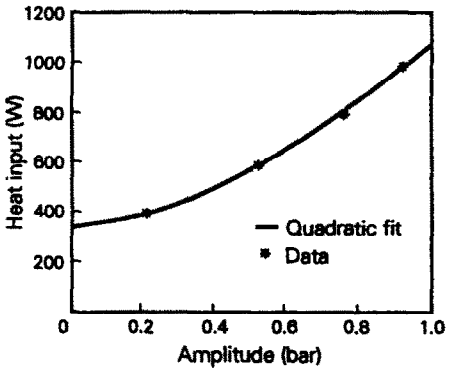


FIG. 4. Variation of the amplitude of pressure-drop oscillations with heat input. Experimental data.

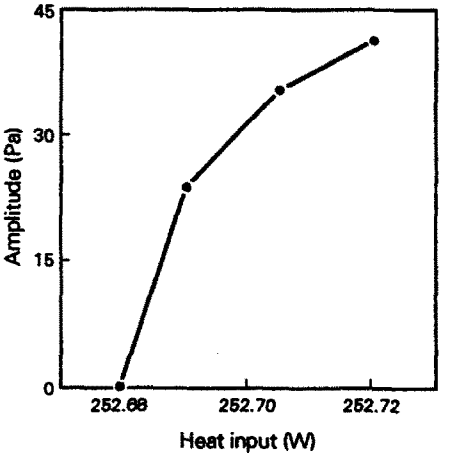


FIG. 5. Variation of the amplitude of pressure-drop oscillations with heat input. Results of integral model close to bifurcation point.

Table 1. Pressure-drop oscillations and Ledinegg instability compared

*Pressure-drop oscillations*
(1) Dynamic instability.
(2) *Conditions*: (i) internal characteristics with negative slope;
(ii) external characteristics steeper than internal;
(iii) compressible volume (e.g. surge tank) in the flow circuit.
(3) Caused by a *Hopf bifurcation* as the heat input is increased.
(4) The standard way to eliminate pressure-drop oscillations is to make the slope of the internal characteristics positive (e.g. by internal throttling).

*The Ledinegg instability*
(1) Static instability.
(2) *Conditions*: (i) internal characteristics with negative slope;
(ii) internal characteristics steeper than external;
(iii) multiple intersections of the internal and external characteristics.
(3) Caused by a *saddle-node bifurcation* as the heat input is increased till the internal characteristics intersect with the external.
(4) The standard way to avoid the Ledinegg instability is to make the slope of the external characteristics steeper than that of the internal.

### 3.3. *Mechanisms of the pressure-drop oscillations and the Ledinegg instability*

We have seen that the pressure-drop oscillations and the Ledinegg instability are both related to the operation of the two-phase flow system on the negative-slope region. However, the crucial difference between the two is caused by the feedback effect of the surge tank, leading to *oscillatory* behavior, as opposed to the *excursive* behavior in the absence of the surge tank. These differences are reflected in the type of bifurcation that takes place at incipient instability. Table 1 and Fig. 6 are developed to highlight these differences. The figures are developed to indicate the steady-state characteristics of the channel (internal) and the pump (external), and also the unstable operating points. They are based on typical values of the parameters used in our experiments, e.g. ref. [5].

## 4. CONCLUDING REMARKS

On the basis of the analysis carried out in this work, we can make the following remarks:

(a) Stability criteria for the pressure-drop oscillations and the Ledinegg instability are derived in terms of the magnitude of the negative slope of the steady-state pressure-drop vs mass flow rate characteristics, and thus are independent of the actual two-phase flow model used.

(b) Pressure-drop limit cycles are generated after a super-critical *Hopf bifurcation* in the dynamics of the two-phase flow system. It is to be noted that an excursive instability similar to the Ledinegg instability can occur at a sufficiently high heat input, even when there exists a compressible volume in the flow circuit.

(c) The Ledinegg instability is a static instability caused by a *saddle-node bifurcation.*

(d) The differences between the pressure-drop oscil-

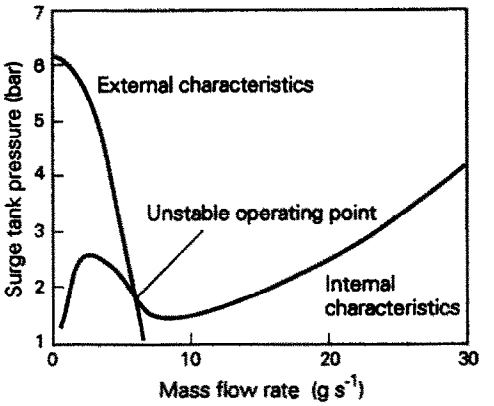


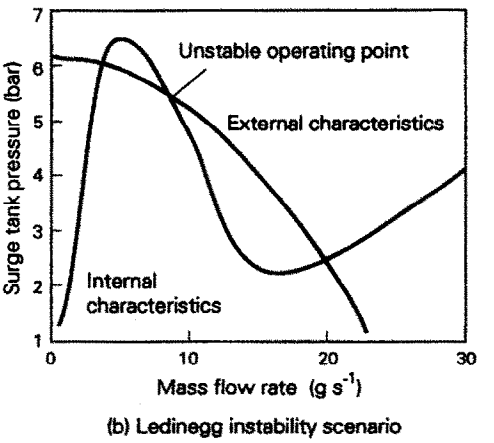


FIG. 6. Schematic diagrams for the instabilities: (a) pressure-drop oscillations scenario; (b) Ledinegg instability scenario.

lations and the Ledinegg instability are reflected in the differences in the type of bifurcation.

*Acknowledgements*—We would like to express appreciation for the help provided by Mr Hongtan Liu in checking the equations, and also for suggesting some useful ideas. This paper was revised and finalized during Dr Kakaç's stay at the Lehrstuhl A für Thermodynamik, Technische Universität München, as the recipient of the Senior Scientists Award from the Alexander von Humboldt Stiftung.

## REFERENCES

1. G. Yadigaroglu, Two-phase flow instabilities and propagation phenomena. In *Thermohydraulics of Two-phase Systems for Industrial Design and Nuclear Engineering* (Edited by J. M. Delhaye, M. Giot and M. L. Riethmuller), Chap. 17. McGraw-Hill, New York (1981).
2. S. Kakaç and T. N. Veziroğlu, A review of two-phase flow instabilities. In *Advances in Two-phase Flow and Heat Transfer* (Edited by S. Kakaç and M. Ishii), Vol. II. Kluwer, Dordrecht, The Netherlands (1983).
3. J. L. Achard, D. A. Drew and R. T. Lahey, Jr., The analysis of linear and nonlinear instability phenomena in heated channels, NUREG/CR-1718, Report prepared for the U.S. Nuclear Regulatory Commission (1980).
4. A. H. Stenning, T. N. Veziroğlu and G. M. Callahan, Pressure-drop oscillations in forced convection with boiling system, *Proc. Symp. on Dynamics of Two-phase Flows*, EURATOM (1967).
5. H. T. Liu, Parametric study of two-phase flow instabilities in a forced-convective boiling upflow system, M.S. Thesis, University of Miami, Coral Gables, Florida (1989).
6. J. Guckenheimer and P. J. Holmes, *Nonlinear Oscillations, Dynamical Systems, and Bifurcations of Vector Fields*, Applied Mathematical Sciences, Vol. 42. Springer, New York (1983).
7. J. M. T. Thompson and H. B. Stewart, *Nonlinear Dynamics and Chaos: Geometrical Methods for Engineers and Scientists*. Wiley, New York (1986).
8. H. N. Shirer (Editor), *Nonlinear Hydrodynamic Modelling: a Mathematical Introduction*, Lecture Notes in Physics, 271, pp. 508–509. Springer, New York (1987).
9. M. Ledinegg, Instability of flow during natural and forced circulation, *Waerme* **61**, 891–898 (1938).
10. R. L. Devaney, *An Introduction to Chaotic Dynamical Systems*, pp. 80–82. Addison-Wesley, New York (1989).

## APPENDIX A. DERIVATION OF THE INTEGRAL MODEL

A.1. *Between the main and surge tanks*

The flow here is single-phase liquid, and the flow is horizontal. Therefore, integration of the momentum equation gives

$$L_1 \frac{dG_i}{dt} = (P_i - P) - K_i \frac{G_i^2}{\rho_l} \tag{A1}$$

where $K_i$ is the combined inlet restriction coefficient, which takes care of the concentrated pressure-drop at the inlet valve, as well as the distributed frictional pressure-drop over the length of the tube.

A.2. *Between the surge tank and system exit*

In this part of the system heat is added, and there is a phase change. Integrating the momentum equation from the surge tank to the system exit, we get the total contributions of different mechanisms to the pressure-drop, i.e. gravitational, accelerational, frictional and the concentrated pressure-drop at the exit restriction, as

$$L_2 \frac{dG_o}{dt} = (P - P_e) - \rho_{av} g L_v - \frac{G_o^2}{\rho_l} \times \left\{ \frac{(1-x_e)^2}{(1-\psi_e)} + \frac{\rho_l x_e^2}{\rho_v \psi_e} - 1 + F_m + \frac{2fL_2}{D} \right\}. \tag{A2}$$

These equations can be looked at from the viewpoint of force-balance. The first term on the right-hand side indicates the *available* pressure-drop, and the rest of the terms indicate the *actual, instantaneous* pressure-drop. The difference between these two—the unbalanced pressure-drop—goes to accelerate the flow.

## APPENDIX B. ANALYSIS OF LEDINEGG INSTABILITY

The so-called Ledinegg instability was first investigated by Ledinegg in 1938 [9]. Here we derive the same result in our notation for easier interpretation. The classical analysis is carried out for a loop similar to that analyzed here; only the surge tank is not present in the loop. Therefore, the equation corresponding to the surge-tank dynamics (equation (2)) is eliminated. In addition, there is only one value of the mass velocity in the system; thus, $G_i = G_o = G$. With this, the two mass velocity equations, equations (1) and (3), can be added—which in effect becomes a complete description of the system—to give

$$(L_1 + L_2) \frac{dG}{dt} = (P_i - P_e) - [K_i + f(G, Q)] \frac{G^2}{\rho_l}. \tag{B1}$$

Linearizing equation (B1), we obtain

$$(L_1 + L_2) \frac{d\delta G}{dt} = \lambda \delta G \tag{B2}$$

where

$$\lambda = -\left[ (K_i + f(G,Q)) \frac{2G}{\rho_l} + \frac{df(G,Q)}{dG} \frac{G^2}{\rho_l} \right]. \tag{B3}$$

The system is stable against infinitesimal perturbations only if $\lambda < 0$, which gives us the condition for stability of the system

$$\left[ (K_i + f(G,Q)) \frac{2G}{\rho_l} + \frac{df(G,Q)}{dG} \frac{G^2}{\rho_l} \right] > 0. \tag{B4}$$

Comparing terms, it can be seen that the nondimensional stability criterion (c) derived in Section 3 is identical to this. Stating this in words, the system is stable if the external characteristics of the pump are steeper than the internal characteristics of the channel, which is a well-known result [1]. To put a finer point on the discussion, this instability may be termed as a 'hydraulic-inertia-controlled' Ledinegg instability (following the terminology in ref. [1]), since the heat input into the fluid is considered to be constant during the excursion.

At incipient instability of this system, the external and internal characteristics are tangent to each other. As the external characteristics become flatter, they cut the internal characteristics at two points, one of which (the 'original' operating point) is unstable, and the other one is stable (see Fig. 6). In the dynamical systems parlance, this bifurcation is known as the tangent or saddle-node bifurcation [7, 10].

## ANALYSE DE BIFURCATION DES OSCILLATIONS DE PRESSION ET INSTABILITE DE LEDINEGG

**Résumé**—Les oscillations de perte de pression et l'instabilité de Ledinegg sont analysées par la théorie des systèmes dynamiques. Une formulation intégrale est développée pour modéliser le système d'écoulement diphasique. Des critères d'instabilité indépendants du modèle actuel d'écoulement diphasique sont dérivés pour les deux phénomènes. On montre que les cycles limites de l'oscillation de perte de pression se produisent après une bifurcation supercritique de Hopf. Dans un prolongement de l'analyse, on tente de clarifier les mécanismes des oscillations de pression et de l'instabilité de Ledinegg. Les deux phénomènes sont classés sous l'angle de la théorie de bifurcation et on souligne les différences.

## BIFURKATION BEI DRUCKVERLUST-OSZILLATIONEN UND DIE LEDINEGG-INSTABILITÄT

**Zusammenfassung**—Die Druckverlust-Oszillationen und die Ledinegg-Instabilität werden vom Standpunkt der dynamischen Systemtheorie untersucht. Zur Beschreibung des zweiphasigen Strömungssystems wird eine integrale Form verwendet. Für beide Phänomene wird ein Kriterium für Instabilität entwickelt, das unabhängig vom aktuellen Zweiphasenströmungs-Modell ist. Es zeigt sich, daß nach einer überkritischen Hopf-Bifurkation die Grenzzyklen der Druckverlust-Oszillation auftreten. In Erweiterung der Analyse werden Anstrengungen zur Klärung der Mechanismen der Druckverlust-Oszillationen und der Ledinegg-Instabilität unternommen. Beide Phänomene werden vom Standpunkt der Bifurkationstheorie klassifiziert; Unterschiede werden herausgearbeitet.

## БИФУРКАЦИОННЫЙ АНАЛИЗ КОЛЕБАНИЙ ПЕРЕПАДА ДАВЛЕНИЯ И НЕУСТОЙЧИВОСТЬ ЛЕДИНЕГГА

**Аннотация**—На основе теории динамических систем анализируются колебания перенада давления и неустойчивость Лединегга. Разработан единый подход к моделированию системы двухфазных течений. Лля двух исследуемых явлений получены критерии неустойчивости, не зависящие от модели реального двухфазного течения. Показано, что предельные циклы колебаний перепада давления наблюдаются за сверхкритической бифуркацией Хопфа. Кроме того, предпринята попытка выяснения механизмов колебаний перепада давления и неустойчивости Лединегга. Дана классификация обоих указанных явлений с точки зрения теории буфуркаций и отмечены различия между ними.